# Atkamine: A New Pyrroloiminoquinone Scaffold from the Cold Water Aleutian Islands *Latrunculia* Sponge

**Yike Zou** and **Mark T. Hamann**

Department of Pharmacognosy, Pharmacology, Chemistry and Biochemistry, School of Pharmacy, University of Mississippi, University, Mississippi 38677, United States

Mark T. Hamann: mthamann@olemiss.edu

## Abstract

A new pyrroloiminoquinone alkaloid, named atkamine, with an unusual scaffold was discovered from a cold, deep water Alaskan sponge *Latrunculia* sp. collected from the Aleutian Islands. Olefin metathesis was utilized to determine the location of the double bond in the hydrocarbon chain. The absolute configuration was determined by using computational approaches combing with the ECD (electronic circular dichroism) spectroscopy.

The pyrroloiminoquinone alkaloids are known for their potent bioactivity toward various types of tumor cell lines[1,2] and with the potential target of mammalian topoisomerase II in vivo.[3] Other bioactivities of this alkaloid class include antimicrobial, antiviral, antimalarial, caspase inhibition, feeding deterrence, and immunomodulatory.[4] These utilities together with the highly strained ring system have attracted a broad range of interests. Several total syntheses of this alkaloid class have been developed, including discorhabdin A,[5] makaluvamine D,[6] and other derivatives.[7] Our discovery efforts searching for novel ring systems from the Alaskan marine region prompted us to focus on the cold water Alaska sponge *Latrunculia* sp. Although new discorhabdin alkaloids were discovered from our previous studies,[8] an assessment of the extracts using LCMS revealed the generation of uniquely different formulas from those previously reported. As a result, from our recollection, a novel-type of pyrroloiminoquinone alkaloid was discovered. We report here a

strained heterocyclic ring system named atkamine[9] and elucidated with the assistance of chemical degradation, NMR, ECD spectra, and computational approaches.

Atkamine was isolated as a green-purple TFA salt soluble in methanol, DMSO, and dichloromethane. HRESIMS showed quasimolecular ions at $m/z$ 734.3006 [M + H]$^+$ and 736.3008 [M + H + 2]$^+$ in a ratio of approximately 1:1.2 generating a reasonable molecular formula of $C_{40}H_{53}BrN_3O_3S$ (± 2.79 ppm). The UV spectrum showed an absorbance band range from 270 to 450 nm with the peak absorbance of 313 and 360 nm referring to a conjugated system. Acquiring from NMR experiments, the structure of the pyrroloiminoquinone motif was retained;[8] the rest of this molecule was changed dramatically from other reported pyrroloiminoquinone alkaloids.[1,4]

Structural elucidation started from a tertiary carbon resonance ($\delta$ 81.1). The attached proton H ($\delta$ 5.42) showed a two-bond HMBC (Figure 1) correlation to C8; two 3-bond HMBC correlations to C7 and C9; and a weak 4-bond "W"-type HMBC correlation to C10, which together demonstrated that C24 was connected to the C8 on the pyrroloiminoquinone core. The chemical shift of C24 ($\delta$ 81.1) and H24 ($\delta$ 5.42) suggested an oxygen attachment. H24 was detected as a singlet by proton NMR with an additional HMBC correlation to a quaternary carbon ($\delta$ 78.3) thus establishing the covalent connection of C24– C23 ($\delta$ 78.3). On the basis of this connection, the other two HMBC correlations of H24 were three-bond correlations to two tertiary carbons, C ($\delta$ 90.2) and C ($\delta$ 69.0), through the ether linkage and through the quaternary C23, respectively. The characteristic chemical shift of C9 ($\delta$ 147.3) indicated an amino substitution on the α-position of the carbonyl group, which was commonly found in pyrroloiminoquinone derivatives.[4–8] This assignment was verified by an HMBC correlation from H ($\delta$ 5.23) to C9; the carbon ($\delta$ 90.2) was thus arranged as C14 connecting to the pyrroloiminoquinone core through N13. This arrangement was also supported by the HMBC correlation from H14 to C24. Fused to the pyrroloiminoquinone core, the 1,3-oxazinane moiety constructed by C8, C9, N13, C14, O14, and C24 was established.

Based on this elucidation, the HMBC correlation from H24 to C ($\delta$ 69.0) must be a 3-bond correlation through the quaternary C23, and C ($\delta$ 69.0) was therefore attached to C23. The tertiary C ($\delta$ 69.0) was demonstrated to be also connected to C14 because H14 showed the HMBC correlations to C23 and C ($\delta$ 69.0). It was therefore elucidated as C15 ($\delta$ 69.0) located between C14 and C23. This arrangement can be verified by the HMBC correlations from H15 ($\delta$ 3.90) to C14 and C24. The bridged seven-membered ring (8-oxa-2-azabicyclo[3.2.1]oct-3-ene) constructed by C8, C9, N13, C14, C15, C23 and C24 was thus assigned.

H15 showed four strong HMBC correlations to a set of aromatic carbon resonances ($\delta$ 108.2, 129.2, 131.0, and 143.2). These data established the connection of C15 to a substituted benzene moiety. The arrangement of the aromatic carbons and substitution pattern of the benzene ring was established first by a key HMBC correlation from H15 to the aromatic C ($\delta$ 129.2). Based on the aromatic proton resonances and HMBC correlations, it was clear that the two sharp singlet resonances H ($\delta$ 7.23s) and H ($\delta$ 6.72s) belonged to the benzene ring and were *para* to each other. According to the chemical shifts, C ($\delta$ 105.3) was shielded and

C ($\delta$ 154.8) was deshielded, which indicated the charge distribution pattern and corresponding bromine and the oxygenated substitution, respectively. The remaining substituted aromatic C ($\delta$ 143.2) was shown to be attached to a sulfur[10] linked to the quaternary C23 ($\delta$ 78.3) based on the HMBC correlation from H15 to C21. The positions of the aromatic carbons were thus arranged as C16 ($\delta$ 131.0), C17 ($\delta$ 129.2), C18 ($\delta$ 105.3), 19 ($\delta$ 154.8), C20 ($\delta$ 108.2), and C21 ($\delta$ 143.2). To secure this arrangement, the HMBC correlations from the aromatic proton H17 to C15; from H20 to C16, C18, C19, and C21; from H14 to C16; and from H15 to C16, C17 and C20 were verified. Interestingly, the aromatic C18 and C20 signals were at unusually high field which referred to highly local negative charge distribution.

From the remaining proton NMR signals, three peak clusters including a deformed triplet of the terminal methyl resonance, $CH_3$ ($\delta$ 0.81 t), a series of overlapped methylene signals, $(CH_2)_n$ ($\delta$ 1.00–1.55), and two overlapped olefinic proton resonances, H ($\delta$ 5.28) and H ($\delta$ 5.30), could be clearly observed. This evidence supported a monounsatu-rated aliphatic side chain. Analyzing the 2D NMR spectra, the isolated spin system on the side chain can be readily deduced. This side chain was attached to the quaternary C23 based on the HMBC correlation from H15 to C25 ($\delta$ 35.1) and the correlations from H25a ($\delta$ 1.76) and H25b ($\delta$ 1.87) to C23. The chemical shifts of the allylic C36 ($\delta$ 26.9) and C39 ($\delta$ 27.0) along with the coupling constant of approximately 10 Hz between the two olefinic protons suggested a Z configuration of the double bond,[11,12] which also matched well with the chemical shift prediction for the allylic carbons (Figure S15, Supporting Information). However, because of the overlapped signals on the aliphatic region, the position of this double bond was difficult to determine by using NMR. This issue was solved by fragmentation using an olefin metathesis (Figure 2).

The spatial relationship of the atoms was established based on the NOESY experiment, and the relative configuration was thus elucidated (Figure 3). From the observed NOESY correlations, it was clear that H14, H15, H24, and C25 were syn to each other, and the heterocycles were all *cis*-fused.

The crystal for an XRD structure of atkamine was unachievable likely due to the limited amount of the sample and the flexible side chain. Alternatively, molecular modeling approaches were adopted. The rigid backbone with high electron density provided atkamine as an ideal candidate for molecular modeling using ab initio calculations. By using computational approaches and ECD experiments, the absolute configuration was determined. The MMFF-minimized structures were optimized in silico by using the hybrid DFT[13] calculations with the B3LYP or BH&HLYP methods with the 6-31G(d,p) or TZVP basis set and the PCM[14] solvation model (Figure 4), respectively, to enhance the reliability. Notably, resulting from the optimized structures, the dihedral angle of H14–C14–C15–H15 was nearly 90°, which explained the undetectable $^3J_{H14–H15}$ on the proton NMR, and this also matched well with the Karplus equation. The optimized structures were then used for the excited-state TDDFT calculations, and the resulted excitation energies and rotational strengths were Boltzmann weighted and fit to a Gaussian function to generate a computed ECD spectrum and subsequently superimposed on the experiment data. Analyzing from the long wavelength region, the computed spectra showed two electronic transitions at 380 and

330 nm which were also recorded by the experiment. This absorption band was elucidated as a set of overlapped signals produced by the $n \rightarrow \pi^*$ transitions from the hetero-atomic substations on the aromatic system. The $\pi \rightarrow \pi^*$ transitions and the aromatic $^1L_b$ transitions at the region of 250–300 nm were a more specific and characteristic presentation of the electronic structure of the conjugated system, and this was also reproduced by the calculations. From the overlaid ECD spectra (Figure 5), the absolute configuration of atkamine was thus assigned as 14*R*,15*S*,23*S*,24*R*.

Atkamine presented a new ring system. Intriguingly, the biogenesis of atkamine likely originates from just two standard amino acids and a monounsaturated fatty acid precursor without rearrangement (Figure 6). A proposed biogenesis is provided in the Supporting Information (Figure S11). Atkamine appears to utilize the common starting material and intermediate from the makaluvamine pathway.[4] It may derive from makaluvamine M, and the aliphatic side chain has possibly originated from (*Z*)-15-docosenoic acid, a primary metabolite which was commonly found in sponge species with abundance.[15] Several key steps included an acylation between the enamine moiety and the FA source,[16] the formation of a quinone methide intermediate,[17] consecutive conjugate additions,[18] and a finally reductive cyclization. The incorporation of the sulfur in vivo is still under investigation, although it was achieved synthetically by nucleophilic addition,[5] and two possible pathways were proposed here.

Atkamine represents a unique pyrroloiminoquinone alkaloid core. The highly fused rings joined with several heteroatoms will provide a synthetically challenging target. The bioactivity of atkamine has not been presented due to the remote collection site and the challenge of sample recovery. A total synthesis will be essential to further investigate the chemistry and effectively characterize the biological potential for this new ring system.

## Supplementary Material

Refer to Web version on PubMed Central for supplementary material.

## Acknowledgments

## References

1. Antunes EM, Copp BR, Davies-Coleman MT, Samaai T. Nat Prod Rep. 2005; 22:62. [PubMed: 15692617]

2. Crews P, Gerwick W, Schmitz F, France D, Bair K, Wright A, Hallock Y. Pharm Biol (Lisse, Neth). 2003; 41:39.

3. Radisky DC, Radisky ES, Barrows LR, Copp BR, Kramer RA, Ireland CM. J Am Chem Soc. 1993; 115:1632.

4. Hu JF, Fan H, Xiong J, Wu SB. Chem Rev (Washington, DC, US). 2011; 111:5465.

5. Tohma H, Harayama Y, Hashizume M, Iwata M, Kiyono Y, Egi M, Kita Y. J Am Chem Soc. 2003; 125:11235. [PubMed: 16220942]

6. White JD, Yager KM, Yakura T. J Am Chem Soc. 1994; 116:1831.

7. (a) Rives A, Delaine T, Legentil L, Delfourne E. Tetrahedron Lett. 2009; 50:1128.(b) Iwao M, Motoi O, Fukuda T, Ishibashi F. Tetrahedron. 1998; 54:8999.(c) Morooka Y, Fukuda T, Iwao M. Tetrahedron Lett. 1999; 40:1713.(d) Izawa T, Nishiyama S, Yamamura S. Tetrahedron. 1994; 50:13593.(e) Wada Y, Otani K, Endo N, Harayama Y, Kamimura D, Yoshida M, Fujioka H, Kita Y. Tetrahedron. 2009; 65:1059.(f) Oshiyama T, Satoh T, Okano K, Tokuyama H. Tetrahedron. 2012; 68:9376.

8. Na M, Ding Y, Wang B, Tekwani BL, Schinazi RF, Franzblau S, Kelly M, Stone R, Li XC, Ferreira D, Hamann MT. J Nat Prod. 2010; 73:383. [PubMed: 20337497]

9. Named after a major Aleutian Island known as Atka Island.

10. This sulfur substitution is commonly found in pyrroloiminoquinone alkaloids.[1,4]

11. Gunstone FD, Pollard MR, Scrimgeour CM, Vedanayagam HS. Chem Phys Lipids. 1977; 18:115. [PubMed: 832335]

12. Bus J, Sies I, Lie Ken Jie MSF. Chem Phys Lipids. 1977; 18:130. [PubMed: 832336]

13. Density functional theory: Kohn W, Sham LJ. Phys Rev. 1965; 140:A1133.Hohenberg P, Kohn W. Phys Rev. 1964; 136:B864.Calais JL. Int J Quantum Chem. 1993; 47:101.In The Challenge of d and f Electrons. Comstock MJ. American Chemical SocietyWashington, DC1989; 394:i.

14. Polarizable continuum model: Pascualahuir JL, Silla E, Tuñon I. J Comput Chem. 1994; 15:1127.Cossi M, Barone V, Cammi R, Tomasi J. Chem Phys Lett. 1996; 255:327.

15. Denis C, Wielgosz-Collin G, Bretéché A, Ruiz N, Rabesaotra V, Boury-Esnault N, Kornprobst JM, Barnathan G. Lipids. 2009; 44:655. [PubMed: 19266225]

16. (a) Denic V, Weissman JS. Cell. 2007; 130:663. [PubMed: 17719544] (b) Jakobsson A, Westerberg R, Jacobsson A. Prog Lipid Res. 2006; 45:237. [PubMed: 16564093] (c) Su HM, Moser AB, Moser HW, Watkins PA. J Biol Chem. 2001; 276:38115. [PubMed: 11500517]

17. Bolton JL, Turnipseed SB, Thompson JA. Chem-Biol Interact. 1997; 107:185. [PubMed: 9448752]

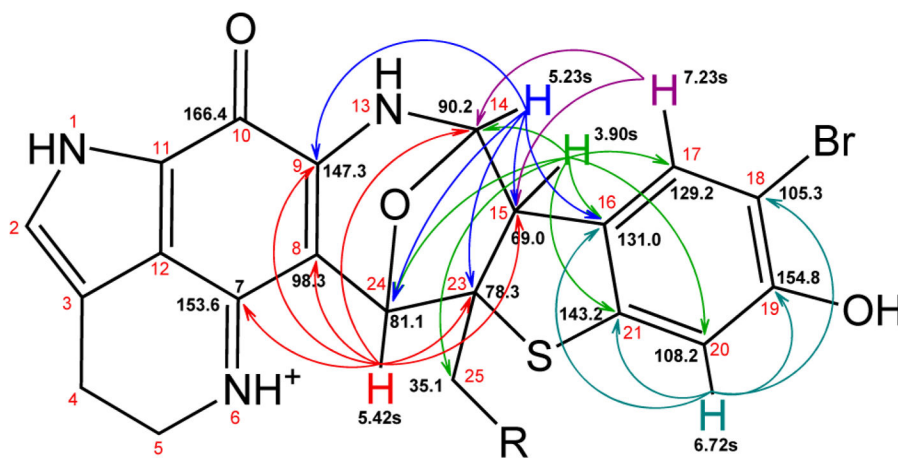18. Begley TP, Xi J, Kinsland C, Taylor S, McLafferty F. Curr Opin Chem Biol. 1999; 3:623. [PubMed: 10508664]

**Figure 1.**
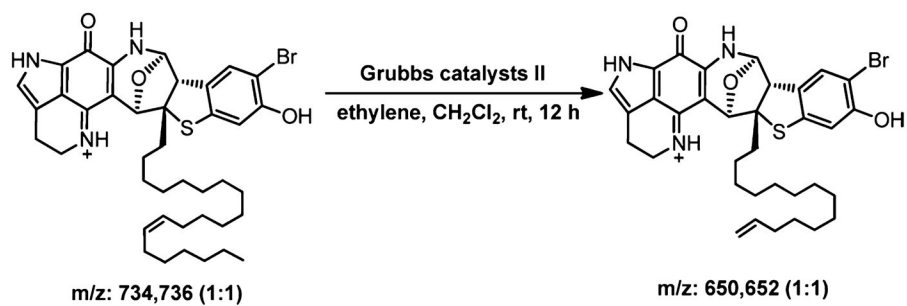Key NMR chemical shifts and HMBC correlations of atkamine (R = FA side chain).

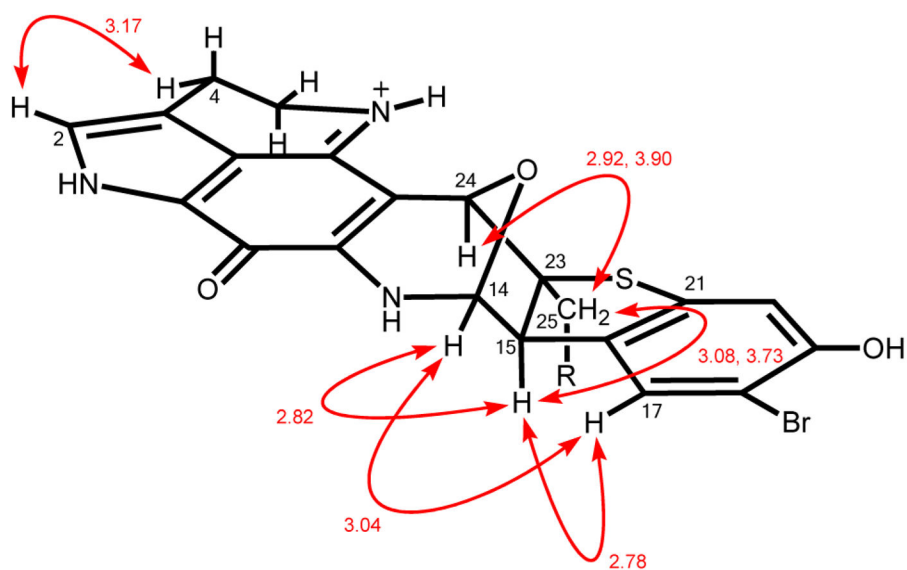**Figure 2.**
Olefin metathesis on atkamine.

**Figure 3.**
Perspective structure and key NOESY correlations of atkamine with calculated distances (red, in angstroms).
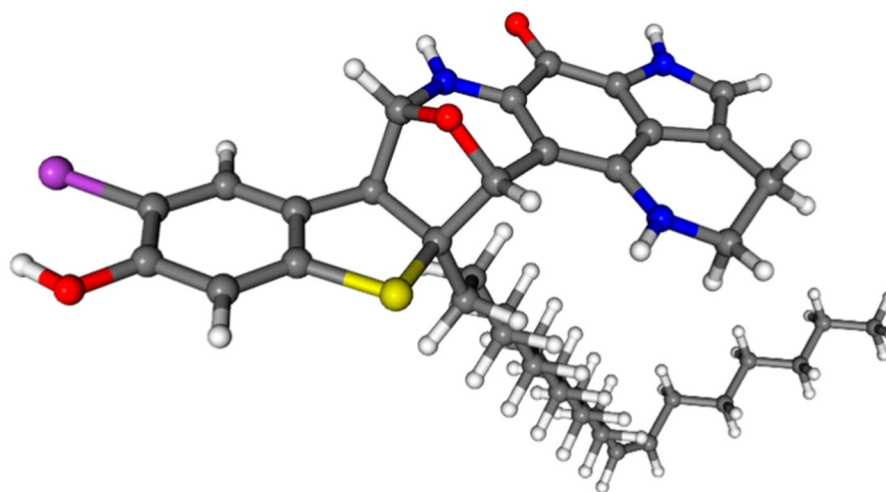
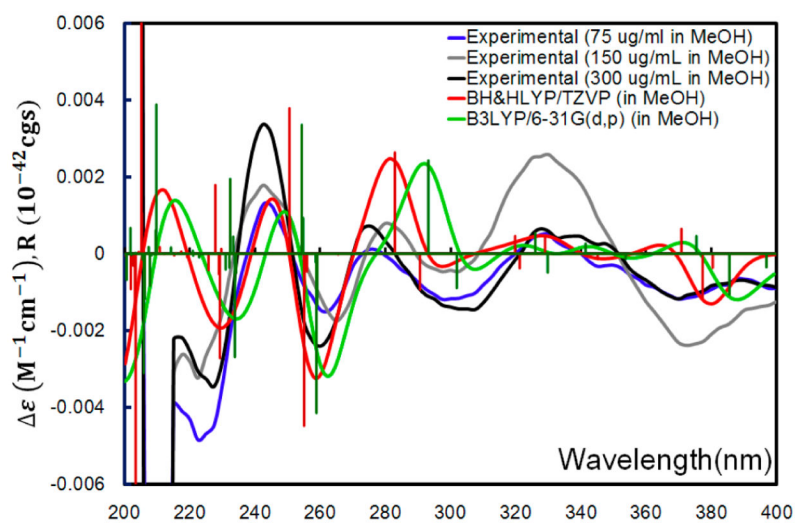**Figure 4.**
DFT-optimized structure of atkamine.

**Figure 5.**
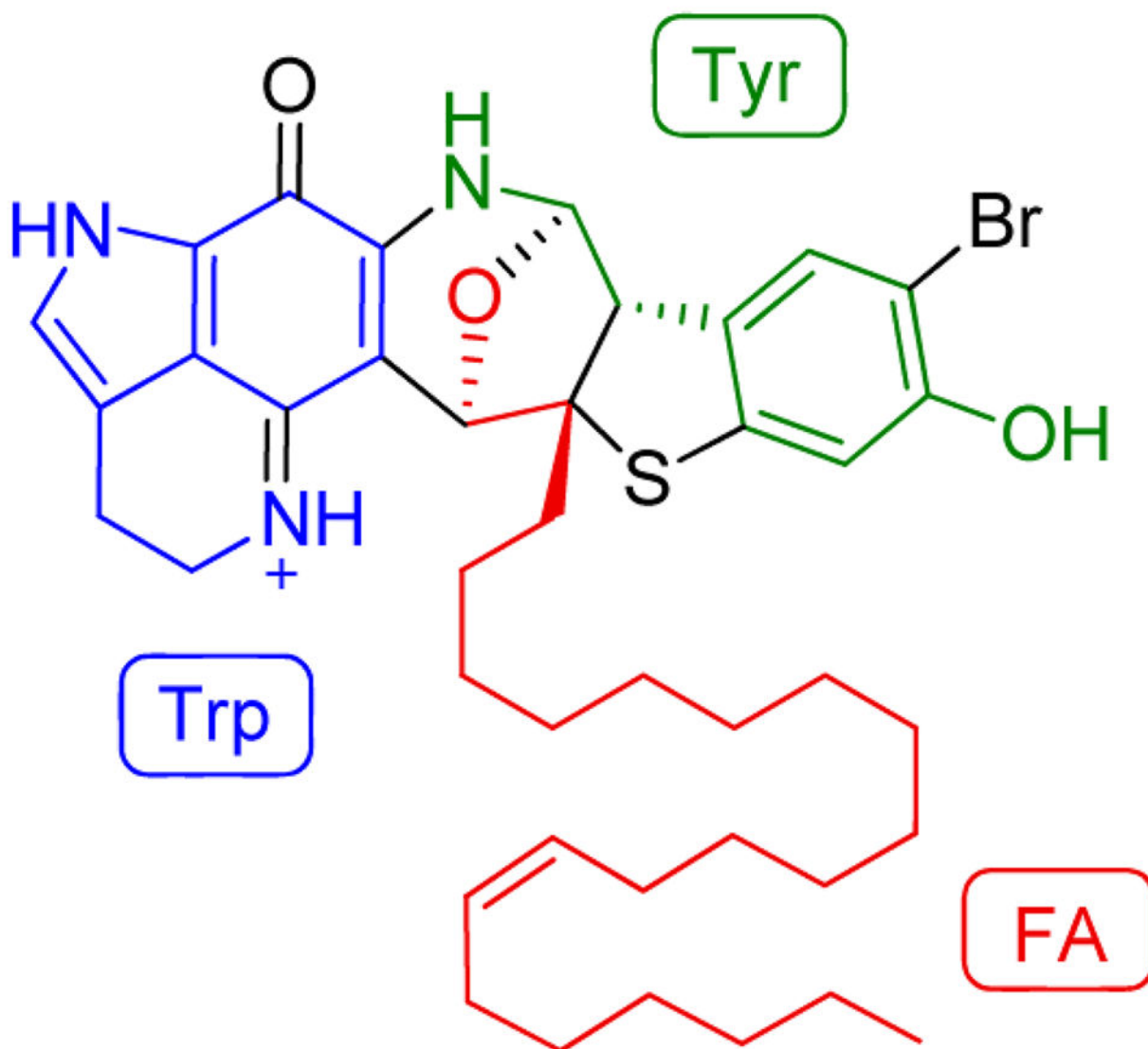Experimental ECD spectra and computed excited states and ECD curves by Boltzmann average.

**Figure 6.**
Core components of atkamine.

*Org Lett*. Author manuscript; available in PMC 2014 August 19.

**Figure 6.**
Core components of atkamine.